PAPER

Searching for a new ionomer for 3D printable ionic polymer–metal composites: Aquivion as a candidate

To cite this article: Sarah Trabia *et al* 2017 *Smart Mater. Struct.* **26** 115029

Smart Mater. Struct. 26 (2017) 115029 (17pp) https://doi.org/10.1088/1361-665X/aa919f

Searching for a new ionomer for 3D printable ionic polymer–metal composites: Aquivion as a candidate

Sarah Trabia, Zakai Olsen and Kwang J Kim

Active Materials and Smart Living Laboratory, Department of Mechanical Engineering, University of Nevada-Las Vegas (UNLV), Las Vegas, NV 89154, United States of America

E-mail: kwang.kim@unlv.edu

Received 7 July 2017, revised 2 October 2017
Accepted for publication 6 October 2017
Published 26 October 2017

CrossMark

Abstract

The work presented in this paper introduces Aquivion as a potential candidate for additive manufacturing of ionomeric polymers for the application of IPMCs. First, Aquivion was characterized and compared with Nafion to show that it has the similar qualities, with the major difference being the ionic conductivity. Ionic polymer–metal composites (IPMCs) were fabricated using off-the-shelf membranes of Nafion and Aquivion. The actuation tests showed improved performance for an IPMC with Aquivion as the base compared to an IPMC with a Nafion base. With these results in mind, additive manufacturing of unique shapes using Aquivion filament was studied. A 3D printer was modified to work with Aquivion filament and the polymer was printed into various shapes. Using the printed membranes, IPMCs were fabricated using an electroless plating process. Nafion-based and printed Aquivion-based IPMCs were tested for their performance in back relaxation, frequency driven actuation, blocking force, and mechano-electric sensing. The printed Aquivion-based IPMCs performed comparably to Nafion-based IPMC in back relaxation and showed significantly improved performance in frequency driven actuation, blocking force generation, and mechano-electric sensing.

Keywords: 3D printing, IPMC, ionomer, aquivion, ionic polymer–metal composite

(Some figures may appear in colour only in the online journal)

1. Introduction

1.1. Basics of ionic polymer–metal composites (IPMCs)

IPMCs for short, are a class of electroactive polymers that have been studied for many years [1, 2]. IPMCs are ionomer-based, typically Nafion, which is then plated with a noble metal. When an electric potential is applied to the surface, the negatively charged side attracts cations, causing it to swell. This swelling of one side forces a bending motion in the IPMC. This soft actuator is ideal for many applications because of its ability to work well in water and low voltage input to high deformation ratio [2–4].

1.2. Potential Applications of IPMCs

1.2.1. IPMCs as bio-medical, bio-mimetic, and robotic actuators. Extensive research has been made on the application of IPMC actuators in the bio-medical, bio-mimetics, and robotics fields. The IPMCs ability to be used as a mechanical gripper, utilizing 2, 4, or 8 IPMC actuators as tweezer and finger like manipulators was successfully demonstrated by Shahinpoor and Kim [3]. It was further demonstrated that rectangular IPMCs could be used as 3D manipulators, linear actuators, micro-catheter guidance tools [3]. Many researchers have developed IPMC based methods for locomotion, including underwater propulsion. Some designs utilize rectangular IPMC actuators as tail fins for swimming fish robots, underwater vehicles, and tadpole robots [3, 5–9], while sheet IPMC actuators have been cut to shape and embedded within a robotic manta ray fin [10]. Segmenting the electrodes of an IPMC has been shown to give more complex articulation in the tail fin actuators of these swimming bio-mimetic robots [11]. The use of both segmented

IPMC electrodes and rectangular IPMCs as joint actuators have also been used to generate contractile and slithering type locomotion [3, 12]. Shahinpoor and Kim also demonstrated the ability to use IPMC actuators as diaphragm pumps and contractile heart compression assistive devices [3, 13].

1.2.2. IPMCs as sensors. The use of IPMCs as sensors is a widely researched subject. A great deal of work can be found on the basic physics and fundamentals of the IPMCs sensing capabilities, electromechanical response, and use as mechanoelectrical transducers can be found in [1, 4, 14–16]. Abdulsadda and Tan showed that an array of IPMC sensors could be utilized as an artificial lateral line, akin to what is found in many aquatic animals, to localize a dipole source [17]. Strazzeri *et al* demonstrated the use of an IPMC as a vibration sensor in a similar fashion to common mass-spring-damper sensor systems [18].

1.3. Traditional fabrication methods for the ionomer base

The fabrication methods of IPMCs are continually advancing, but many of the traditional techniques are still used to construct these actuators and sensors. An overview of some traditional fabrication processes demonstrates the wide range of possible techniques for creating the ionomer membranes, all of which are applicable to IPMC manufacturing. Nafion is typically available in sheet form from the manufacturer. This is useful for cutting out generic shapes, such as rectangles. There are a variety of thicknesses (ranging from 25.4 to 254 μm) available for purchase depending on what the user would like. This has been used a variety of ways, including cutting the sheets to mimic fins [19, 20]. Extrusion of ionomer materials has been shown to be a useful technique for IPMC fabrication [21], and the method has been used to fabricate Nafion tube multi degree of freedom IPMC sensors [22]. The fabrication done by Palmre *et al* with hot-pressing [23] and Stalbaum *et al* with extrusion [22] further demonstrated the use of precursor pellets for thermal processing of the ionomer materials for IPMCs. Hot pressing may also be used to combining multiple membranes by compressing them together under high temperature to create a single, fused membrane. Injection molding is another thermal processing method shown to work with ionomer materials by Nelson [21]. Injection molding takes precursor pellets to mold a membrane of specified thickness and geometry. Dispersions of ionomer materials have been successfully used to manufacture IPMCs through film casting techniques. In this technique, a water dispersion of the ionomer material is cast as layers into a mold and dried or thermally cured [24]. This method can also be used to construct IPMCs by casting an ion conducting electrode solution, thus eliminating the need for the post processing of electrode coating [25].

1.4. Advanced fabrication methods for the ionomer base

Though the traditional fabrication methods have been able to solve many problems, Nafion is an expensive material and the current methods have limited the shapes that can be made. Researchers have been looking for solutions to find ways to reduce the amount of Nafion used as well as creating new, intricate shapes to expand the actuation motions possible. Blending techniques have been presented that mix Nafion with a cheaper polymer to create the base for IPMCs. Hwang *et al* has blended Nafion water dispersion with poly(vinyl alcohol-*co*-ethylene) (PVA-*co*-E) to produce membranes that were produced using a casting method [26]. They found a ratio between the two polymers (30:70, PVA-*co*-E:Nafion) that still had the advantageous characteristics of Nafion and was able to produce IPMCs that were able to perform just as well as full Nafion IPMCs, while reducing the amount of Nafion being used. Nam *et al* blended Nafion water dispersion with polyamic acid (PAA), which is a precursor for polyimide (PI) [27]. These blends were also cast to produce the membranes. They showed that a ratio of 18:82 (PI:Nafion) was ideal, producing IPMCs that were comparable to that of full Nafion membranes. These two studies have shown the potential to reduce the amount of Nafion used in IPMCs without losing the desired characteristics and abilities of Nafion and IPMCs. The ability to produce different shapes has been recently explored. Since creating intricately shaped membranes is difficult with the current fabrication methods, spray-painting Nafion water dispersion has been introduced to solve this. Trabia *et al* were able to produce Nafion membranes using vinyl stencils and an airbrush [28]. The produced shapes retained the detailed outlines of the stencils, as well as voids within the membrane if desired. The freedom of producing stencils allows the user to be able to produce any shape at a needed thickness using this method. The IPMCs produced with these membranes have been shown to actuate comparable to that of traditionally made IPMCs.

Additive manufacturing (3D printing) has been on the forefront of many research areas today. Carrico *et al* have shown that this method of manufacturing is possible with Nafion [29, 30]. They designed a 3D printer to work with filament that they have produced in-house. The shapes printed with their system are not possible, or could be very difficult to produce, using traditional methods. They were able to print parts for a soft robot that can crawl along a tube and a torsional actuator that can twist [30]. Their system has allowed researchers to potentially create complete robots by simply drawing their design in a computer-aided design program and a 3D printer.

2. Objectives

As previously discussed, Nafion is usually the ionomer used for IPMCs. As mentioned, Nafion is a good option for IPMCs, but the material has some issues in heat processing techniques. This study proposes to introduce another option

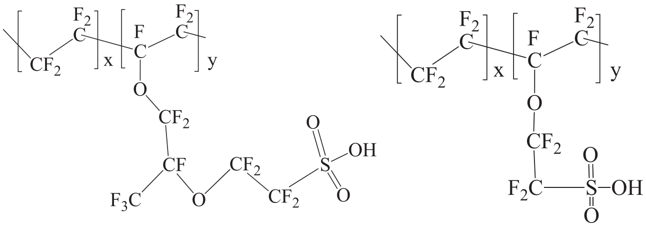

Nafion **Aquivion**

Figure 1. Polymer structure for Nafion (left) and Aquivion (right) membranes comparing the side chain lengths.

for additive manufacturing of ionomers: Aquivion. This ionomer has a shorter side chain, similar material properties, and nearly double the ionic conductivity of Nafion (figure 1). To show that Aquivion is a viable option, the objectives of this research is to fully analyze and compare off-the-shelf Nafion and Aquivion membranes, then produce printed Aquivion shapes.

3. Approaches

To complete the objectives for this research, the following approaches are presented. A complete material characterization of Nafion and Aquivion membranes was conducted to show that the two are comparable. IPMCs were produced using the commercially membranes and performance testing will be conducted. For 3D printing Aquivion ionomers, the physics of additive manufacturing and 3D printer design is discussed. The procedure for filament production and 3D printing is presented. Material characterization of the printed samples is conducted to show that the samples are similar to off-the-shelf membranes and are not contaminated or affected by the process. The printed samples are activated and plated with platinum. Printed Aquivion IPMCs produced undergoes performance testing and a comparison to Nafion based IPMCs.

4. Methods

4.1. Comparing Nafion and Aquivion

An IRTracer-100 (Shimadzu) was used to compare chemical structure for Fourier transform-infrared spectroscopy (FT-IR). To identify the thermal degradation temperature, a thermogravimetric analyzer (TGA), specifically the Q500 (TA Instruments) was used. The thermal conductivities of the two polymers were measured using a TCi thermal conductivity meter (C-Therm).

The ion exchange capability of the ionomers is verified by an ion exchange capacity (IEC) test. The membrane samples (2 cm × 2 cm) were dried in the oven at 80 °C overnight. The samples were then weighed and the dry mass was recorded. The dried membranes are soaked in 50 ml of 1 M of sodium chloride (NaCl, Sigma-Aldrich) overnight. A drop of phenolphthalein (Sigma-Aldrich) is added to the solution and then it is titrated with 0.01 M of sodium hydroxide (NaOH, Sigma-Aldrich) until the solution is light pink. The volume of NaOH used is recorded for each sample. To find the IEC for each, the following equation is used:

$$\mathrm{IEC} = \frac{VC}{M_{\mathrm{dry}}},$$

where V is the volume of NaOH used in ml, C is the concentration of the titrant (0.01 M) and M_{dry} is the dry mass of the membranes in grams. Three samples of each membranes were tested. To view the samples fabricated, a scanning electron microscope (SEM, TM3030 Hitachi) at 15 kV was used. For the samples viewed in the SEM, they were set in resin and the surface was polished. The surface was then sputtered with platinum for about 10 s.

4.2. Filament production and 3D printing of Aquivion

As discussed by Carrico *et al*, fused filament fabrication, a type of additive manufacturing, requires polymer filament that can be extruded during the manufacturing process [29]. This filament is produced by melt processing a pelletized form of the polymer through the same method as seen in commercial filament production. The pelletized polymer is fed through a channel by a feed auger. At the far end of the channel, a high temperature zone is created which melts the polymer, which allows for extrusion through a die of specified diameter. Here, a small-scale filament production unit, the Noztek Pro, was used to process Aquivion precursor pellets into filaments of 2 and 3 mm diameter. Once manufactured, the Aquivion filament was used in appropriately modified 3D printers. Carrico *et al* thoroughly discussed the challenges of printing of ionomer materials, specifically Nafion, and how they were able to overcome the various issues in the manufacturing process [29]. Two 3D printing platforms, the Raised 3D N2 Plus and Lulzbot Mini, have been adapted to address the added complications and work with ionomer materials, such as Aquivion. The Raised 3D N2 Plus is a medium format 3D printing system with a 12 × 12 × 24 in. build volume, whereas the Lulzbot Mini is small format platform with a 6 × 6 × 6 in. build volume. Each of these printers had to undergo different modifications in order to print Aquivion. The Raised N2 Plus features a fully constrained 1.75 mm diameter filament path, which is known to play an important role in the printing of ionomer materials [30] and will be discussed further in a later part of this paper. Additionally, this system has a hot end that is capable of reaching 280 °C, another key component to ionomer printing. To modify this printer to use Aquivion a high temperature build platform was installed. This new heated build platform consisted of a 10 × 10 in flexible silicone heating pad (McMaster-Carr) with a 10 W in^{-2} power output density which is insulated on its lower surface with a borosilicate glass plate (McMaster-Carr) placed on its upper surface. The constrained filament path of this printer is not exactly 1.75 mm but is in fact closer to 2 mm. This diameter should be matched as closely as possible to reduce the possibility of filament buckling.

Table 1. Cleaning process procedure for various points in the plating process.

Bath	Supplier	Temperature and time
3 wt% hydrogen peroxide (H_2O_2)	Sigma-Aldrich	65 °C, 45 min
1 M of sulfuric acid (H_2SO_4)	Sigma-Aldrich	65 °C, 45 min
DI water	Filtered in lab (Millipore)	65 °C, 45 min
DI water	Filtered in lab (Millipore)	65 °C, 45 min

The Lulzbot Mini is a smaller 3D printing system that has the ability to be upgraded to a different filament extruder. To address the issues of hot end temperatures and the constrained filament path, a Lulzbot Flexystruder mini was installed onto the Lulzbot Mini. The Flexystruder utilized a fully constrained 3 mm filament path and allows for maximum hot end temperatures of 280 °C. This extruder is also specifically designed work with flexible materials, being fitted with deeper grooves in the pinch roller feed mechanism. The deep grooves reduce the possibility of filament slipping, which plays an important role in additive manufacturing physics. Similarly to the Raised N2 Plus, a 6 × 6 in flexible silicone heating pad (McMaster-Carr) with 10 W in^{-2} power density and a borosilicate glass plate (McMaster-Carr) was installed. In both systems, the glass plate was coated with double sided Kapton tape to further promote bed adhesion, which is important to achieving high quality prints, as discussed by Turner *et al* [31].

4.3. Activation and platinum plating

The Aquivion precursor pellets are put through a hydrolysis process, to 'activate' the membranes. This process exchanges the current end group (sulfonyl fluoride group) to a sulfonate end group, allowing the Aquivion to be able to conduct ions and carry water molecules with them. To do this, the membranes are suspended in an aqueous solution of 15% of potassium hydroxide (KOH, Sigma-Aldrich), 35% of dimethyl sulfoxide (DMSO, Sigma-Aldrich), and 50% deionized water (DI water, Millipore) at 75 °C with proper stirring, until the samples have been activated fully. This process depends on the thickness of the membrane as Elliot *et al* have mentioned in their studies [32]. After the activation process, the membranes are ready to be platinum plated by using the procedure detailed by Kim and Shahinpoor [33]. An electroless plating process is used for the samples fabricated. The cleaning process is summarized in table 1. Hydrogen peroxide removes the organic impurities, while the sulfuric acid removes the metallic impurities.

The primary plating process begins with the samples sitting in a platinum salt bath ($Pt(NH_3)_4Cl_2{\cdot}H_2O$, tetraammineplatinum(II) chloride hydrate, Sigma-Aldrich) for 3.5 h, where they are flipped every half hour. The primary plating process follows where the samples are suspended in 350 ml of DI water bath and 0.3 ml of ammonia (NH_3, Sigma-Aldrich) with 0.2 grams of sodium borohydride ($NaBH_4$, Sigma-Aldrich) added every half hour for a total of two hours. The solution is mixed at 130 rpm and it begins at 50 °C with the temperature is increased by 2 °C every half hour. After, the membranes are cleaned by a similar process to that in table 1, excluding the hydrogen peroxide bath. This whole process is repeated two more times. The secondary plating process uses a bath with 0.25 grams of the platinum salt and 0.3 ml ammonia in 350 ml of DI water, stirred at 90 rpm and heated to 50 °C. The samples are suspended in this solution and two solutions are added every half hour for a total of four hours: 2 ml of hydroxylamine hydrochloride ($H_2NOH{\cdot}HCl$, Sigma-Aldrich) and 1 ml of hydrazine ($NH_2NH_2{\cdot}H_2O$, Sigma-Aldrich). The temperature is increased by 2 °C every half hour as well. The membranes are rinsed off by DI water and the surface resistance is measured to ensure that both sides are between 1 and 3 Ω. If it is higher than this range, the secondary plating process is repeated and the surface resistance is measure again. Once this is between the designated range, the membranes are cleaned using the process shown in table 1, excluding the hydrogen peroxide. Finally, the samples are placed in a 1 M of LiCl bath for the ion exchange process for 24 h.

4.4. IPMC performance testing

For the IPMC performance characterization tests, four tests were conducted: back relaxation, actuation, blocking force, and sensing. The signal for all three was generated with a signal generator (SDG1025, Siglent) and a power amplifier was also used (LVC-608, AE Techron). For back relaxation and actuation tests, the displacement was measured using a laser displacement sensor (optoNCDT-1401, Micro-Epsilon), shown in figure 2. For the blocking force tests (figure 3), the force generated by the IPMC was measured using a load cell (GSO-30, Transducer Techniques). The data was collected with a Data Acquisition system (SCB-68, National Instruments) and LabVIEW was used to plot the data of the different values being collected as the test was being conducted and save the data at the end of a test. For the sensing experiments, an electrodynamic shaker (VR-5200, Vibration Research Corporation) moves an IPMC that is clamped at one end (figure 4). The data is sent through a custom amplification circuit, then collected using a Data Acquisition system (USB-6008, National Instruments) and LabVIEW.

5. Results and discussion

5.1. Comparing Nafion and Aquivion

Nafion and Aquivion are both perfluorosulfonic acids (PFSAs), with a Teflon-like backbone. Nafion has a

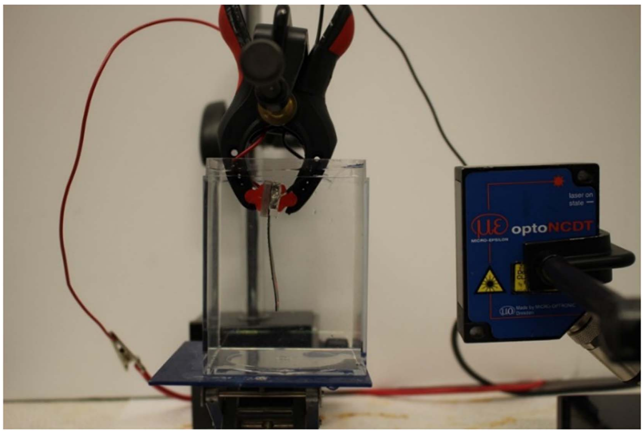

Figure 2. IPMC actuation test setup (for both back relaxation and frequency-based displacement) with a laser sensor performed in DI water.

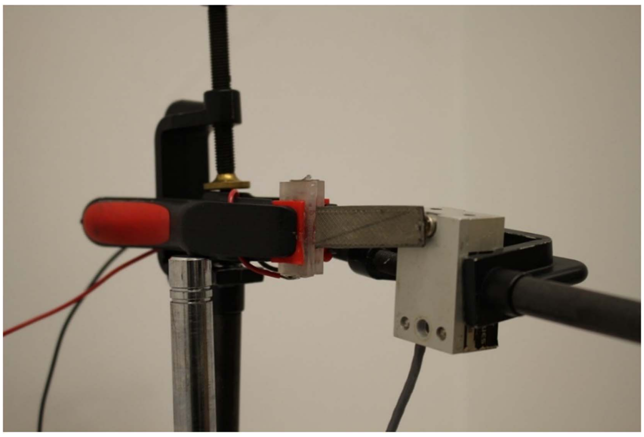

Figure 3. IPMC performance testing for blocking force capabilities in air.

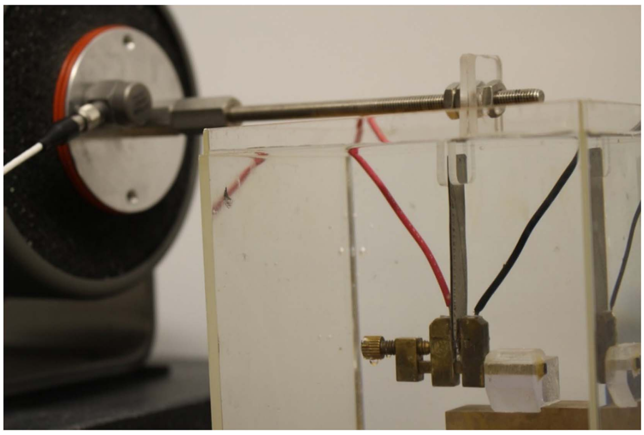

Figure 4. IPMC performance sensing test conducted in DI water.

perfluorovinyl ether side group and a sulfonate end group. Aquivion has a shorter side group: sulfonyl fluoride vinyl ether. This short side chain gives the polymer a lower equivalent weight, potentially creating a higher ionic conductivity than Nafion. They have comparable Young's moduli and water uptake (table 2). For the precursor pellets, the melting temperature of Aquivion is lower than that of Nafion pellets. The key points to take away from these comparisons is that Aquivion has approximately double the ionic conductivity. Before IPMCs were made using the purchased membranes, the two polymers were characterized in-house. The two membranes are compared with an FT-IR to verify their chemical structure. They both have the same peaks at 1213, 1153, and 1060 cm^{-1}, which correlates to the symmetric CF_2, asymmetric CF_2, and SO_3 bonds (figure 5). These peaks have been confirmed by various researchers [34–37]. The thermal degradation temperature was found to be the same for both ionomers with a TGA (figure 6) and matches what has been noted by other researchers [34, 35, 37–41]. To understand the capability of each membrane to hold ions, IEC tests were conducted. The samples tested showed Nafion to be as expected (0.98 meq g^{-1}), while Aquivion had a higher IEC value (1.25 meq g^{-1}) (table 3) [47]. This value gives some insight to Aquivion's potential ability to perform better than Nafion. The thermal properties of the two polymers are important to understand because of the 3D printing process. Understanding how the pellets are affected by heat can help optimize the print settings, including the nozzle temperature, feed rate into the melt zone, and printer speeds. Samples of Nafion and Aquivion precursor pellets were tested for their thermal conductivities. Samples were made by hot pressing 3 grams of pellets to about 0.35 mm thick sheets. The samples were tested with DI Water as the contact agent and a 500 gram weight on top to ensure there is complete contact with the sensor. Table 4 shows the results from the tests. The value for Nafion matches what was recorded by Khandelwal and Mench [42]. The Aquivion samples had a higher thermal conductivity than Nafion, showing that it is able to conduct heat better than Nafion. This helps during both the filament extrusion and 3D printing processes.

For IPMC fabrication, Nafion 115 and Aquivion E87 were used because they have comparable thicknesses (0.127 mm and 0.120 mm, respectively). The two ionomers were produced into IPMCs using the same electroless plating procedure and the samples were viewed in the SEM. The two are indistinguishable in the SEM images shown in figure 7. Comparing the electrodes, both of the samples show a roughened surface, as well as good contact with the platinum (figure 8). However, it is important to note that for these samples, N-IPMC has a thicker electrode than A-IPMC (~10 μm versus ~5 μm).

The samples are tested for their actuation capabilities with an input of 3 Volts at various frequencies: 100 mHz, 500 mHz and 1 Hz. The slowest applied voltage is 3 Volts at 100 mHz (figure 9). The samples actuated similarly, however when comparing the two displacements, it can be seen that A-IPMC had a larger peak to peak amplitude and faster response times (table 5). The next signal applied to the IPMC samples was 3 Volts at 500 mHz (figure 10). The difference between the peak to peak amplitudes between N-IPMC and A-IPMC has decreased compared to the displacements in the previous test, but the A-IPMC is still actuating further and faster than the N-IPMC (table 6). The last test is an applied voltage of 3 Volts at 1 Hz, which is the fastest signal

Table 2. Characteristics of Nafion [43] and Aquivion [44, 45, 47].

	Molecular weight of side chain ($g\ mol^{-1}$)	Equivalent weight (EW, $g\ eq^{-1}$)	Ionic conductivity ($mS\ cm^{-1}$)	Young's modulus, 50% RH, 23 °C (MPa)	Water uptake	Melting temp. (Pellets) (°C)
Nafion	330.10	1100	100	249	38 wt%	~290
Aquivion	199.08	840	>228	250	30 wt%	230–260

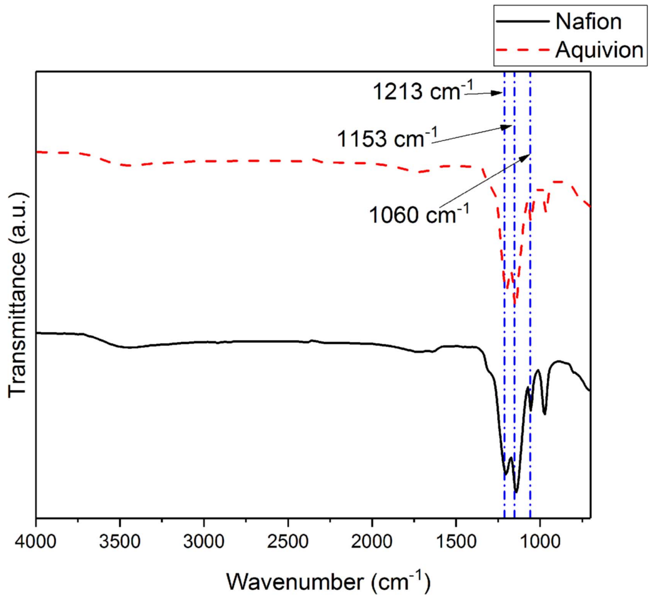

Figure 5. FT-IR comparison of Nafion 115 and Aquivion P87S membranes.

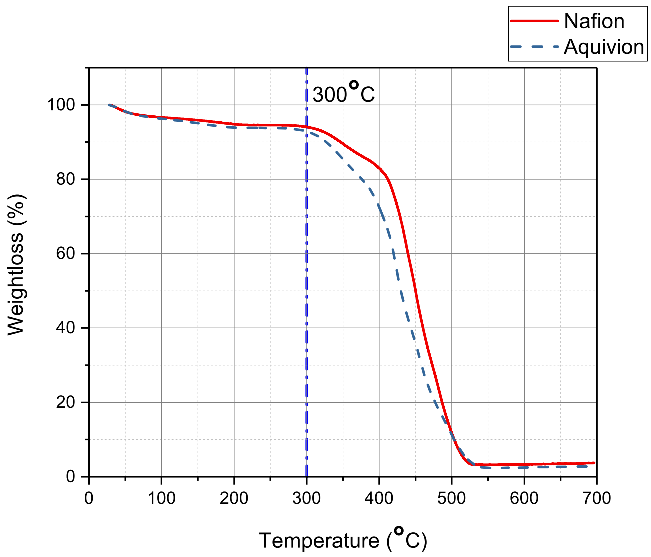

Figure 6. TGA results of Nafion 115 and Aquivion P87S membranes for the thermal degradation temperature.

Table 3. Measured ion exchange capacity results for Nafion 115 and Aquivion E87.

	Ion exchange capacity (meq g^{-1})
Nafion 117	0.98 ± 0.08
Aquivion E87	1.25 ± 0.01

Table 4. Thermal conductivities for Nafion 1100 and Aquivion P87S.

	Thermal conductivity (W mK^{-1})
Nafion 1100	0.289 ± 0.001
Aquivion P87S	0.308 ± 0.002

(figure 11). Typically, 1 Hz is quite a fast signal for an IPMC and the material is not able to reach its maximum displacement. Here it can be seen that the difference between the two peak-to-peak amplitudes has decreased even more so, but again the A-IPMC is still out performing the N-IPMC (table 7). Overall, A-IPMC has larger peak to peak amplitudes and faster response times compared to N-IPMC. In the case of blocking force capabilities, these IPMCs are very thin and it was not possible to test them as they cannot produce a large enough force to be measured by the load cell. The blocking force tests will be conducted on the printed samples versus a Nafion -based IPMC of similar dimensions. The power input of the IPMC samples were plotted and the results are shown in figure 12. At 500 mHz, both samples use about the same amount of power. At the slowest frequency, N-IPMC draws more power than the A-IPMC, while in the fastest frequency, this is reversed. This can be explained by the difference in ionic conductivity between the two samples. A-IPMC has a higher ionic conductivity so it does not need as much power to move the ions in the slowest case. However, in the fastest case, A-IPMC is able to move more ions to the other side than N-IPMC so it requires more power to move them back to the opposite end.

5.2. Filament production

The filament made for these studies was made using Aquivion P87 precursor pellets. The filament extruder, the Noztek Pro, was set to 230 °C and allowed to reach temperature before turning on the motor for the feed auger. This filament extruder is at a 45° angle, helping the pellets and filament move easily. The pellets are filled into the hopper and the motor is turned on, moving the pellets towards the heating zone. It is very important to ensure that the pellets do not have any moisture absorbed because this can cause partial hydrolysis, bringing issues when the filament is being used in the 3D printer. This can be done by either storing the Aquivion pellets in a desiccator or drying the pellets in a vacuum oven at 105 °C for 20 h, as described by Solvay. The diameter of the filament that can be produced are 2 mm and 3 mm. The filament produced is of similar color to the pellets and shows no signs of degradation (figure 13).

5.3. 3D printing Aquivion

5.3.1. Additive manufacturing physics and 3D printer designs. Though there are many 3D printers available, finding a printer that works well for Aquivion, or Nafion as discussed by Carrico *et al* [29], can be difficult. Aquivion filament is relatively soft compared to ABS or PLA filaments, which causes issues such as buckling or the drive gear tearing into the filament. The rate that the filament is fed through is very important as well to ensure that the filament is evenly and thoroughly heated. The nozzle's offset from the printer bed surface can cause too much pressure in the system, which in turn can cause buckling and clogging issues. These are the key issues to keep in mind when designing a 3D printer for either Aquivion or Nafion. Compared to typical plastic

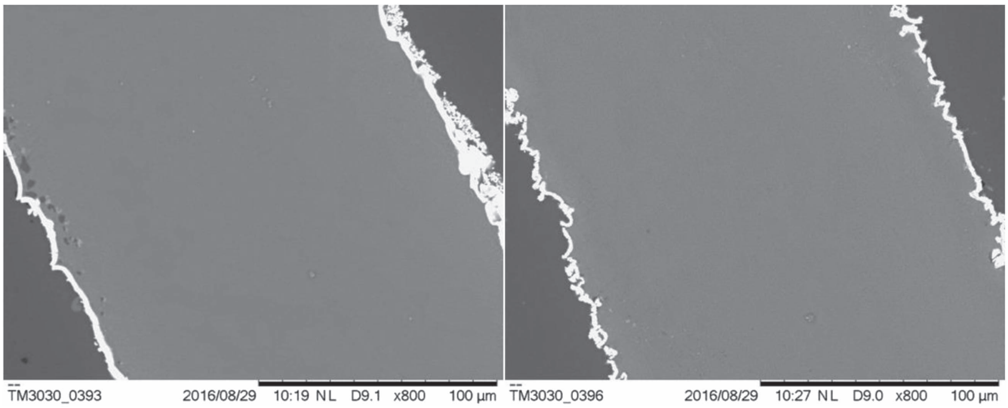

Figure 7. SEM images at a magnification of x800 of N-IPMC (left) and A-IPMC (right).

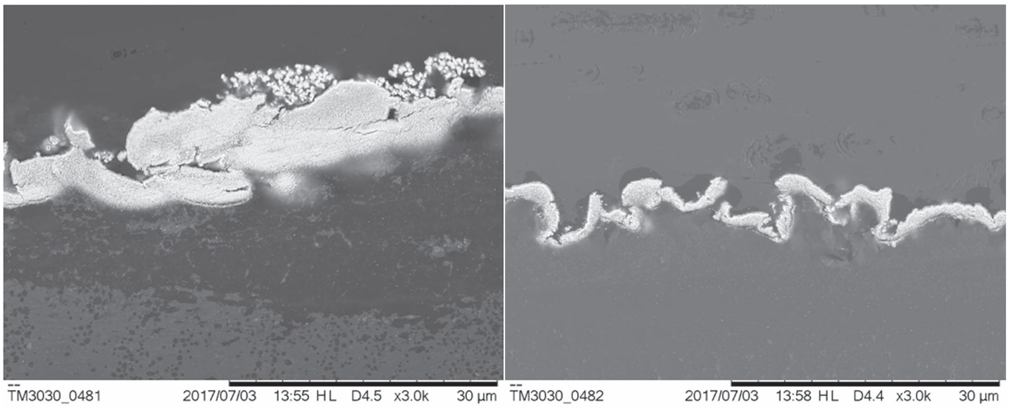

Figure 8. SEM images at a magnification of x3000 of N-IPMC (left) and A-IPMC (right).

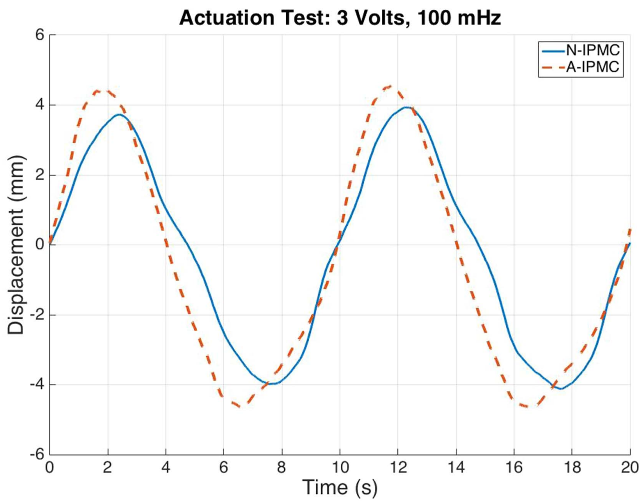

Figure 9. Actuation test results with 3 Volts at a frequency of 100 mHz applied.

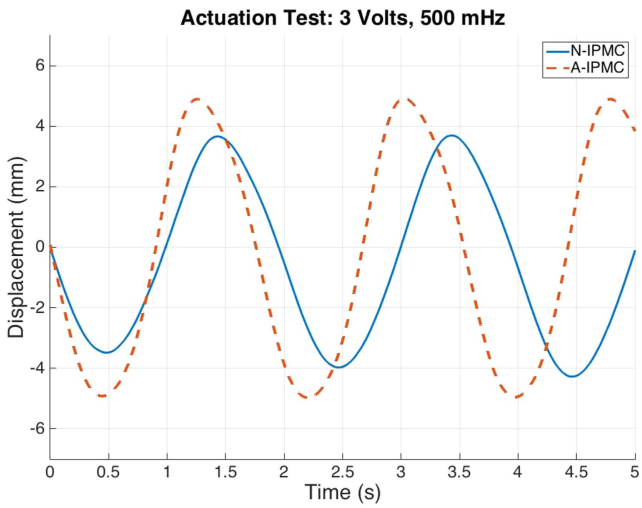

Figure 10. Actuation test results with 3 Volts at a frequency of 500 mHz applied.

filaments that are used in 3D printing, Aquivion and Nafion have higher melting temperatures. To be able to print with these ionomers, the nozzle temperature needs to be at least 260 °C. Though the Aquivion precursor pellets have a melting temperature of 230 °C, after the first thermal treatment during filament extrusion, the material has become 'annealed' in a way so it is not able to melt at the lower temperature. In order to print with the filament, the printer has to be able to reach and hold a high temperature. In the case of printing Aquivion, 260 °C is the ideal extruder temperature. The other side of this issue is having a hot bed that is hot enough to encourage bed adhesion. The hot bed on commercially available printers is not able to reach high enough temperatures (usually 110 °C is the maximum temperature) for the material to adhere to the

Table 5. Details of the analysis from the plots in figure 9.

3 Volts, 100 mHz			
		Response time (s)	
	Peak to peak amplitude (mm)	Time to first peak	Time to second peak
N-IPMC	6.32	2.34	5.4
A-IPMC	11.02	1.79	4.78

Table 6. Details of the analysis from the plots in figure 10.

3 Volts, 500 mHz			
		Response time (s)	
	Peak to peak amplitude (mm)	Time to first peak	Time to second peak
N-IPMC	7.14	0.48	0.95
A-IPMC	9.82	0.44	0.82

Table 7. Details of the analysis from the plots in figure 11.

3 Volts, 1 Hz			
		Response time (s)	
	Peak to peak amplitude (mm)	Time to first peak	Time to second peak
N-IPMC	2.55	0.28	0.49
A-IPMC	3.11	0.25	0.49

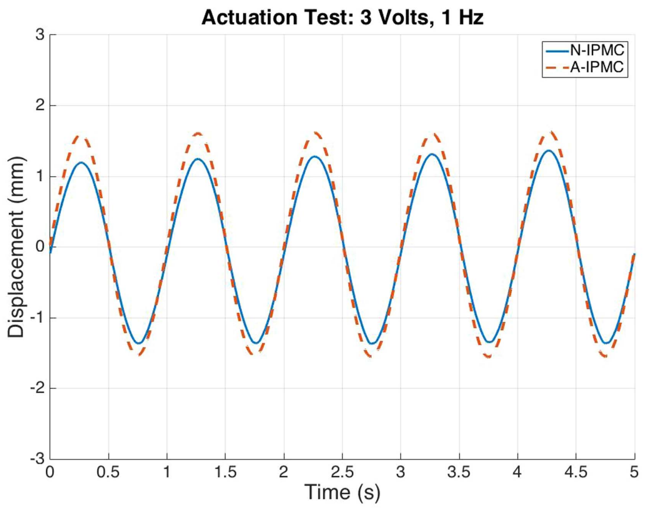

Figure 11. Actuation test results with 3 Volts at a frequency of 1 Hz applied.

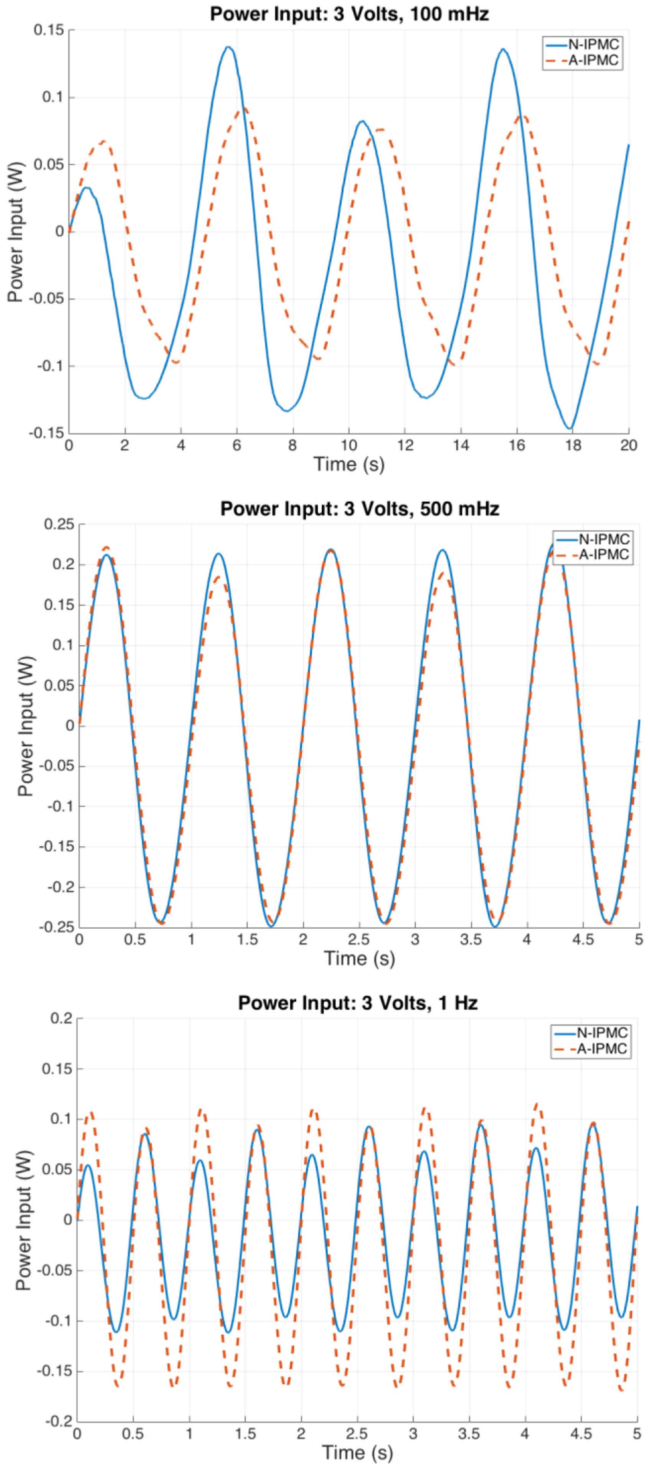

Figure 12. Power input for the three cases of input. From top to bottom, 3 Volts at 100 mHz, 3 Volts at 500 mHz, and 3 Volts at 1 Hz.

bed. Since the extruder temperature is relatively high compared to most materials, the hot bed needs to be close in temperature to reduce the temperature drop after the material has exited the nozzle. The ideal temperature found to encourage bed adhesion is around 180 °C.

Turner *et al* thoroughly presents the physics of additive manufacturing [31]. Some key points were gathered that have helped explain and solve issues encountered. Aquivion filament has shown to be a sensitive material to moisture. If not stored in dry environment, the filament will absorb moisture from the air and partially hydrolyze during the printing process. This causes the filament to become unable to melt, leading to clogging and inability to adhere to the bed surface. A main key point from Turner *et al* that was applied very well to issues with printing Aquivion was the equation

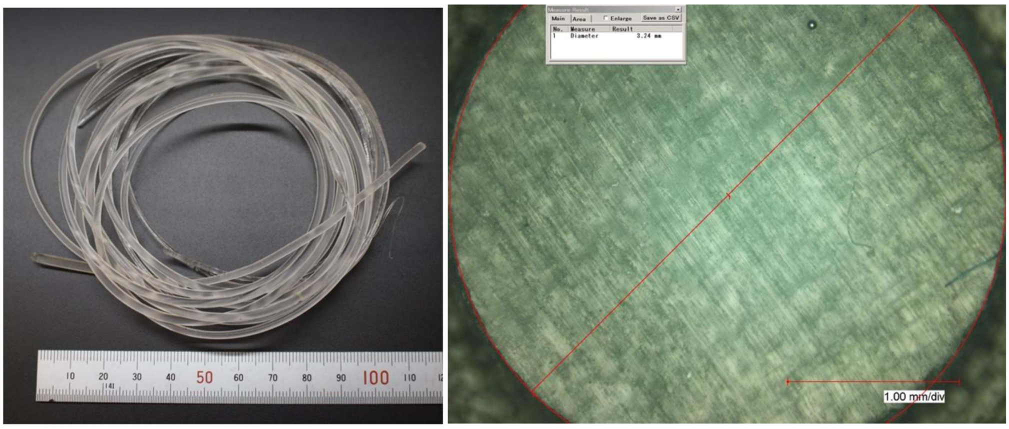

Figure 13. Aquivion precursor pellets drawn into filament (left) and cross-sectional view of the filament with measurement showing the diameter to be around ~3 mm (right).

Table 8. Filament's Young's modulus [44] and dimensions (measured directly from printers in-house) used for the calculations using equation (1) to find the critical pressure for each printer.

	Raised 3D extruder	Flexystruder
Elastic modulus (MPa)	250	
d_f (mm)	2	3
L_f (cm)	10.8	6.35
P_{cr} (kPa)	53	344

for critical pressure. The critical pressure is represented as:

$$P_{cr} = \frac{\pi^2 E d_f^2}{16 L_f^2}, \quad (1)$$

where E is the elastic modulus of the filament, d_f is the diameter of the filament, and L_f is the distance from the drive gear to the entrance of the liquefier [31]. This value denotes the limit of the pressure that can be applied to the filament before it buckles. In fused filament deposition systems, the filament is pushed through the system by a drive gear. The distance between the drive gear and the entrance of the liquefier has shown to be important in successfully printing a soft filament such as Aquivion. Initially, the printer being used was the Raised 3D N2 Plus printer. This printer was chosen because the entire path for the filament is constrained. However, this did not solve the issues of buckling. As shown in equation (1), the distance between the drive gear to the entrance of the liquefier needs to be as short as possible to increase the pressure built within the extrusion setup. In the Raised printer, this distance is about 10.8 cm (4.25 inches) diameter of the filament is 2 mm, resulting in a critical pressure of 53 kPa. Though it is possible to successfully print with this 3D printer, the pressure drop across the melt zone and nozzle exceeded this relatively low critical pressure, and thus filament buckling lead to unreliable printing. To lessen some of the pressure built up within the extruder system, the nozzle diameter was increased to 2 mm. This allowed for a few prints to be successful, but it was not as consistent as a typical 3D printer. A commercially available extruder that is designed to extrude flexible material, the Flexystruder, was purchased and added to the Lulzbot Mini. The distance between the drive gear and the entrance of the liquefier is 6.35 cm (2.5 inches) and the diameter of the filament is 3 mm, giving a critical pressure of 344 kPa. With this new extruder, the system is able to operate at 6.5 times more pressure drop than the Raised extruder, greatly reducing the likelihood of filament buckling. It is possible to keep the nozzle diameter as is (0.5 mm) and produce quality prints. Table 8 summarizes the dimensions measured off the 3D printers and values used for the calculations, as well the calculated critical pressure.

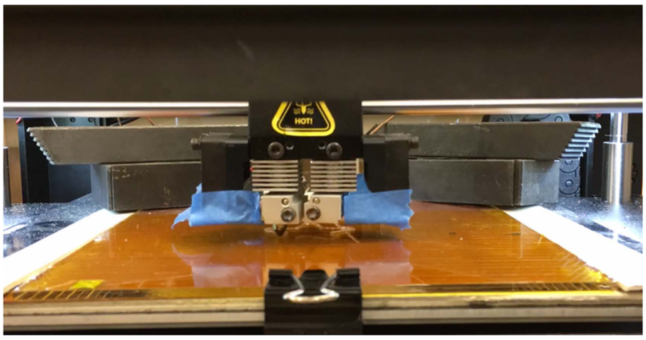

Figure 14. Aquivion filament printed onto double-sided Kapton tape using the Raised N2 Plus Printer.

5.3.2. 3D printing Aquivion samples. The Raised 3D printer systems use the company's proprietary software, ideaMaker, to slice and process STL models. A settings profile was created specifically for Aquvion which included slower printing speeds to minimize back pressure in the nozzle and the use of a brim to promote bed adhesion. Ultimately, the profile was made to print 0.2 mm layers at a default speed of 5 mm s^{-1} and a 120% infill flow rate with 60% overlap and 100% infill. The first layer was printed at 10 mm s^{-1} and 160% flow rate to establish a sturdy foundation for the consecutive layers. The nozzle was set to 260 °C and the hot bed was set to 180 °C. The hot bed was covered with double sided Kapton tape to encourage bed adhesion (figure 14). The samples printed had even thicknesses and good layer adhesion (figures 15 and 16). Similarly, a profile was made

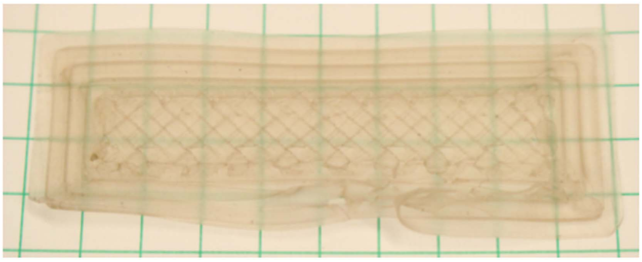

Figure 15. Printed Aquivion in a rectangular shape with a brim to help with bed adhesion (each square on the grid is 6 mm × 6 mm).

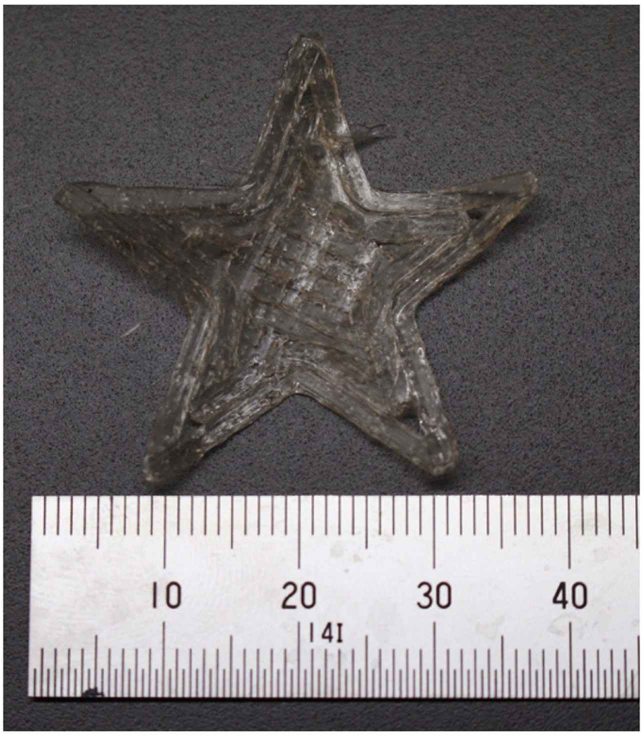

Figure 16. Star-shaped Aquivion membrane printed on the Raised N2 Plus Printer.

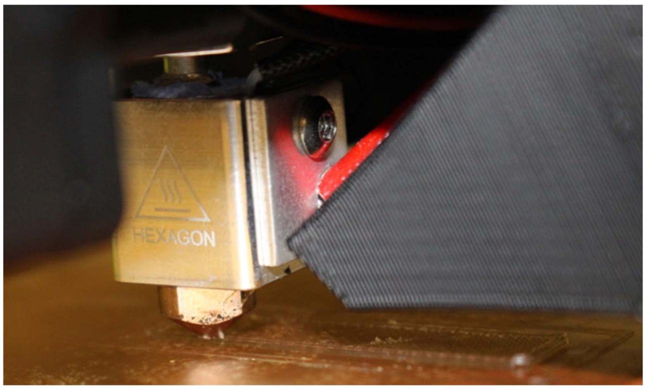

Figure 17. Aquivion printed with the Lulzbot Mini and Flexystruder.

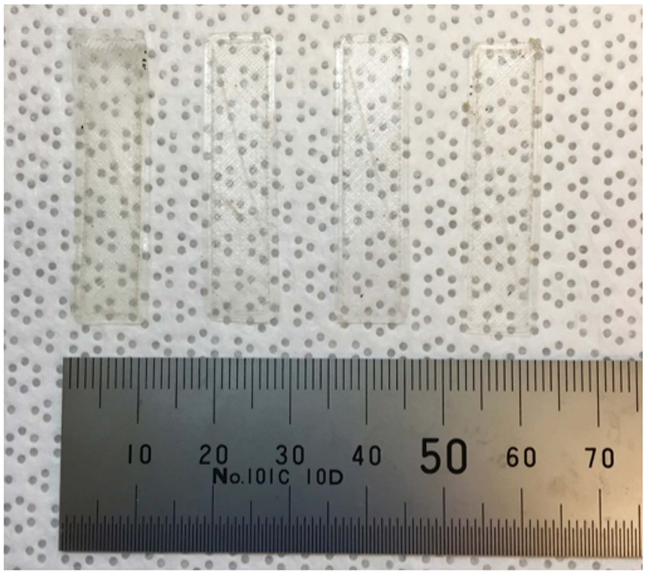

Figure 18. Four Aquivion membrane samples printed using the Lulzbot Mini with the Flexystruder.

to operate the Lulzbot Mini printer with Aquivion. This printer used Cura (Lulzbot Edition) as the slicer, and the profile used similar settings. A 10 mm s^{-1} default print speed was used, along with a 100% first layer flow rate. Due to the larger filament diameter and shorter distance between drive gears and extruder nozzle, the Lulzbot profile did not require as many precautions to limit the filament back pressure. The nozzle was set to 260 °C and the hot bed was set to 180 °C to keep the temperature difference between the nozzle and bed as low as possible. The hot bed has a layer made out of polyetherimide (PEI), which helps with bed adhesion for typical printing materials. This was successful for Aquivion but double sided Kapton tape worked as well. The Lulzbot Mini was able to print the Aquivion filament consistently with good layer adhesion (figure 17). Four samples were printed in sequence and shown in figure 18 with minimal differences in dimensions.

5.4. Material characterization of the printed Aquivion

To ensure that the printed Aquivion sample was not contaminated, it was compared to a pure Aquivion precursor pellet using the FT-IR (figure 19). The two had the same peaks that correlate with the polymer's chemical composition. A sample from the printed Aquivion was tested in the TGA to identify the thermal degradation temperature and compare to that of an Aquivion precursor pellet. The results are compared in figure 20 and it can be seen that the printed sample is able to withstand a higher temperature than the pellet (380 °C compared to 300 °C). This is probably because the ionomer has gone through two thermal treatments and has 'annealed'. After the printed samples were activated, they were compared using the FT-IR to an Aquivion membrane (figure 21). The two have the same peaks at 1213, 1153, and 1060 cm^{-1} corresponding to the symmetric CF_2, asymmetric CF_2, and

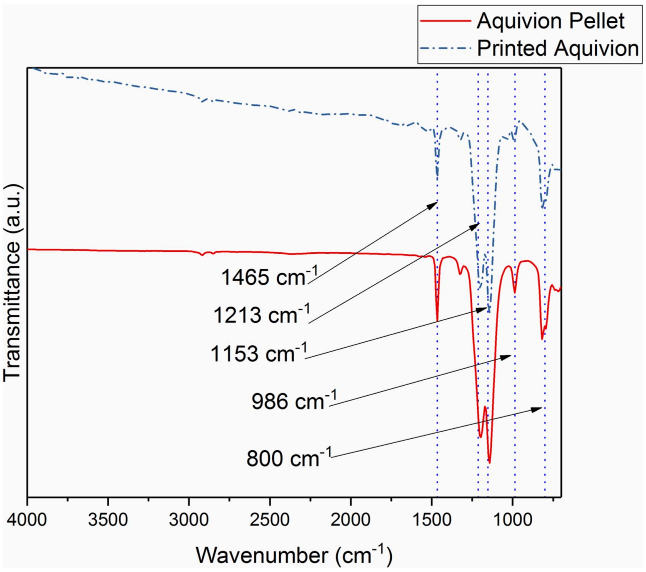

Figure 19. Printed Aquivion sample chemical structure compared with an Aquivion precursor pellet using FT-IR results. Each wavelength correlates to a specific bond that is present in the polymer: 1465 cm^{-1} represents the C–F bond, 1213 cm^{-1} represents the symmetric CF_2 bond, 1153 cm^{-1} represents the asymmetric CF_2 bond, 986 cm^{-1} represents the C–F_3 bond, 800 cm^{-1} represents the S–O bond.

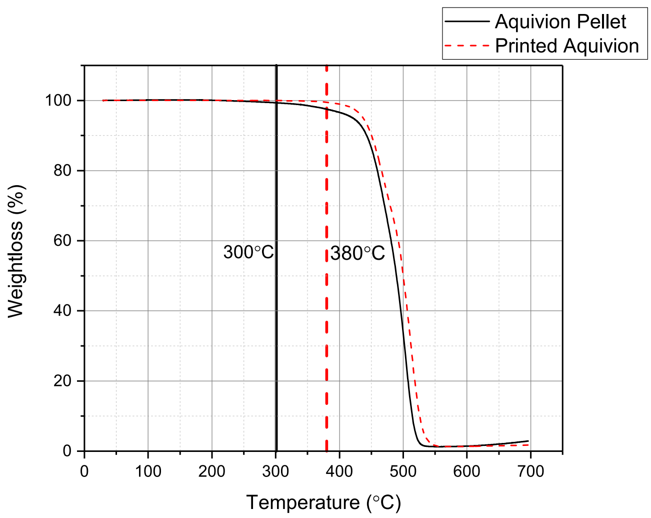

Figure 20. TGA results for the thermal degradation temperature of the printed Aquivion and an Aquivion precursor pellet.

SO_3 bonds. The activated, printed membrane and the Aquivion membrane were tested for their dynamic mechanical properties using the DMA in an environment of relative humidity of about 25% at room temperature. The samples had comparable Young's Moduli (figure 22, left). The printed Aquivion sample has a slightly higher Young's modulus, but should not cause issues in actuation. The damping coefficient, however, differs between the two samples (figure 22, right). When comparing the two samples, the printed Aquivion has a lower damping coefficient, indicating less viscoelastic behavior. The printed Aquivion is not as able to efficiently dissipate the energy absorbed. This could be because of the layering effect during the printing process, stiffening the

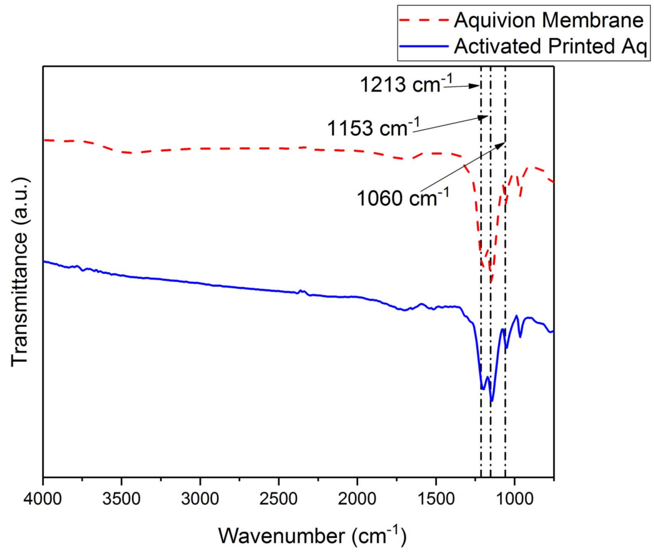

Figure 21. FT-IR results for the chemical structure of activated, printed Aquivion and an Aquivion membrane.

membrane, causing it to not be able to absorb as much vibration as the off-shelf-membrane. However, the difference overall is minimal, when comparing the phase shifts between the two samples (such as 5.3° at 0.1 Hz).

5.5. IPMC performance comparison

The printed Aquivion IPMCs (Pr-Aq-IPMC, figure 23) is compared to traditionally made, Nafion-based IPMC (N-IPMC). Table 9 shows the similar dimensions and surface resistances of the IPMC samples. It is important to compare samples that are as close as possible in shape, since the geometry of the IPMC can affect its performance greatly. The first point of interest was the back-relaxation capabilities. This phenomenon occurs when a DC voltage is applied to an IPMC, forcing it to move to a maximum displacement, until it begins to move backwards to a different position than it initially started. The information from this test gives researchers an idea of how far an IPMC will displace until it no longer can as well as the position it returns to. The displacement is measured for analysis, including calculating the strain. Using the displacement data, the radius of curvature (ρ_r) is calculated using equation (2), where L is the length of the sample and δ is the displacement recorded by the laser displacement sensor. Once that is calculated, it is used to find the strain ε using equation (3), where h is the thickness.

$$\rho_r \cong \frac{L^2 + \delta^2}{2\delta}, \tag{2}$$

$$\varepsilon \cong \frac{h}{2\rho_r}. \tag{3}$$

Overall, the Pr-Aq-IPMC samples were able to actuate further than the N-IPMC (figure 24). They also respond faster than the N-IPMC. The strains produced are within the typical ranges for an IPMC. Between the Pr-Aq-IPMC samples, they were able to perform well between each other.

IPMCs are typically used in frequency-based applications. To determine how well the IPMCs respond to a

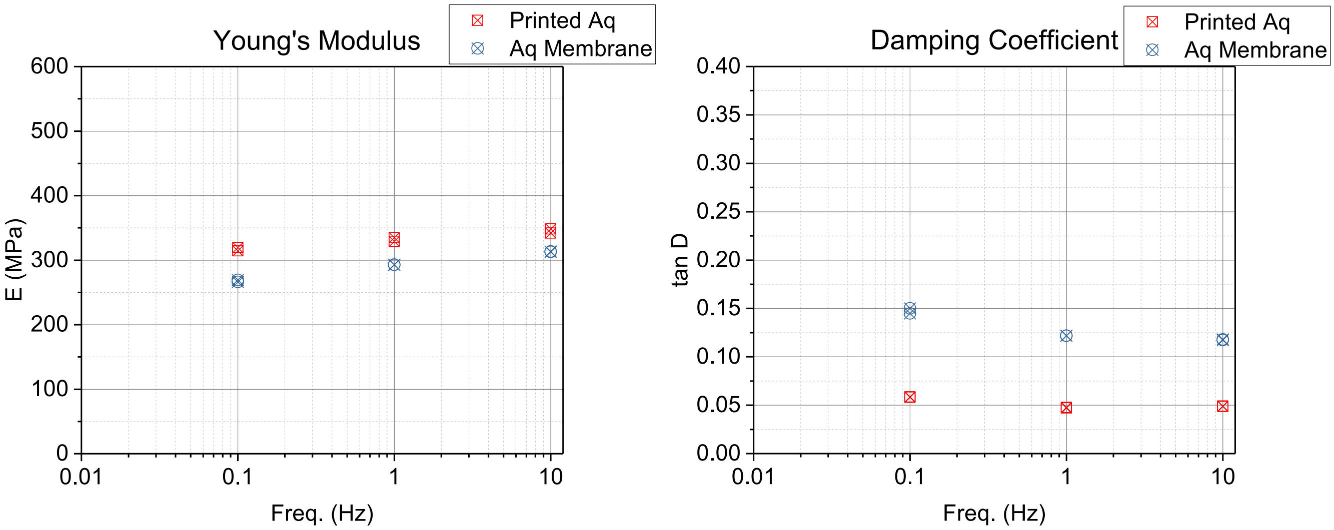

Figure 22. DMA results for activated, printed Aquivion compared with an Aquivion membrane.

Figure 23. Four printed Aquivion IPMCs (Pr-Aq-IPMC) plated with platinum using the electroless plating process (top) and surface of one of the samples at 100x magnification (bottom).

sinusoidal voltage signal, the samples were placed in a DI water-filled tank with 3 Volts at 500 mHz applied. Figure 25 shows the results measured from the tests. Pr-Aq-IPMC samples perform better than the N-IPMC and similarly to each other. A frequency response test was conducted to further investigate the response performance of the samples. From figure 26, it can be seen that the Pr-Aq-IPMC samples all responded faster compared to N-IPMC, within the same amount of time. The Pr-Aq-IPMC samples are all able to produce relatively large displacements, even at 5 Hz, which is considered a fast input for this smart material. This is most likely due to its high ionic conductivity ($\sim$228 mS cm^{-1}) [44, 45]. The final test that was conducted was the blocking force. The samples were tested in air in order to be in contact with the load cell. The samples were completely hydrated before the test was conducted. The input voltage was -1 Volt DC. From figure 27, Pr-Aq-IPMC samples generated a much higher blocking force than the N-IPMC before back relaxation occurs. The stress was calculated by using a dividing the measured force by the cross-sectional area of the IPMC. Both of the samples produce comparable stresses within the IPMC. The volumetric energy density was calculated by taking the peak blocking force value multiplied by the distance the IPMC sample displaced, divided by the free moving volume (table 10). Overall, the Pr-Aq-IPMC samples have higher energy densities than the N-IPMC. When compared to other smart material actuators, a paper written by Shankar *et al* includes a summary plot of various actuators and it can be seen that the IPMC samples presented here perform below what is predicted [46]. This could be because the IPMCs tested for the plot could be thicker or of a different base.

The last test for IPMC performance characterization was the mechano-electric sensing test. The samples were oscillated with a sine wave of 3 mm (peak to peak) at a frequency of 2 Hz. From figure 28, it can be seen that the N-IPMC performs as expected, while the Pr-Aq-IPMC samples vary from sensing close to N-IPMC to almost double that of the N-IPMC sample. The printed IPMCs show promise of introducing new shapes, similar to that of nature's sensors, that can push the field of biomimicry forward.

Overall, the performance of the Pr-Aq-IPMCs have shown promise in their application compared to that of the N-IPMC. There are some differences in their responses which

Table 9. Dimensions of IPMC samples being tested.

	Length (mm)	Width (mm)	Thickness (mm)	Surface resistance (Ω)
N-IPMC	45.08	11.57	0.67	3, 3
Pr-Aq-IPMC 1	45.28	11.08	0.67	2, 2
Pr-Aq-IPMC 2	46.04	11.55	0.68	2, 2
Pr-Aq-IPMC 3	45.66	11.44	0.64	2, 2
Pr-Aq-IPMC 4	45.55	11.07	0.66	2, 2

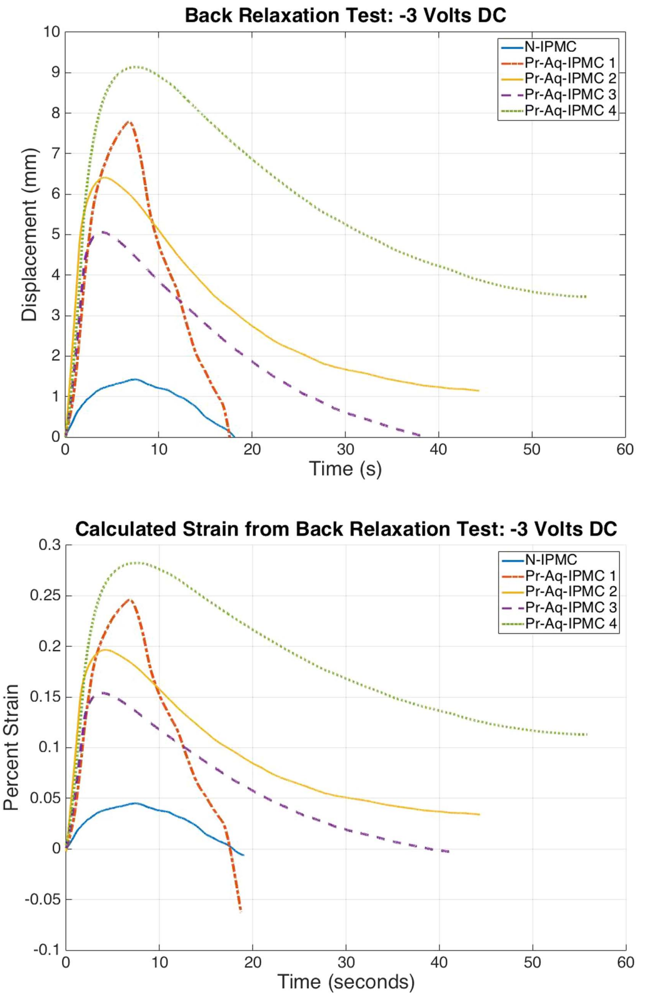

Figure 24. Back relaxation test for the IPMC samples with an applied voltage of −3 Volts DC (top) and the calculated strain from the results (bottom).

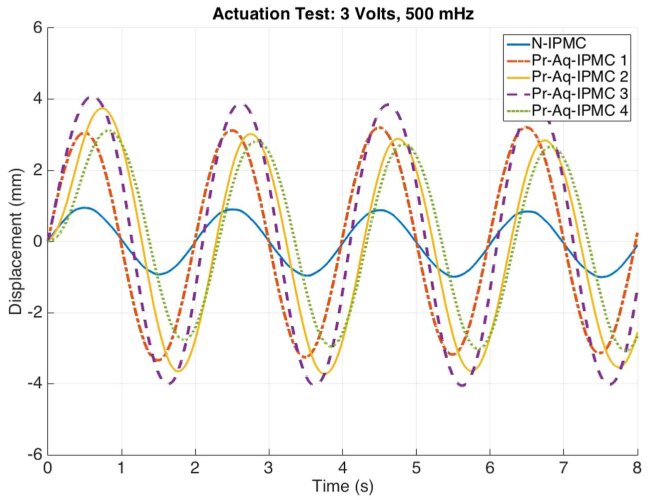

Figure 25. Actuation tests for the IPMC samples at 3 Volts, 500 mHz.

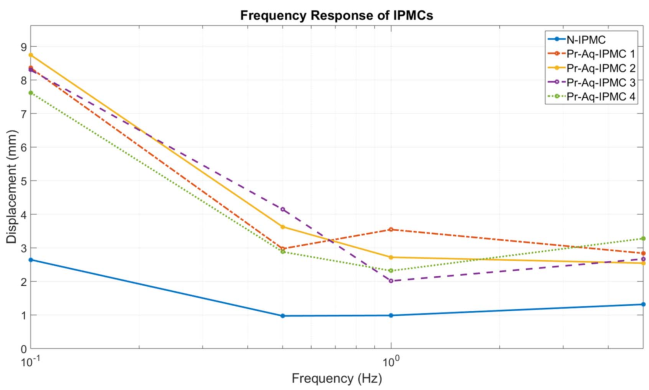

Figure 26. Frequency response plot at 3 Volts driven at 0.1, 0.5, 1, and 5 Hz.

Table 10. Calculated volumetric energy density for the samples.

	Volumetric energy density (J m^{-3})
N-IPMC	9.6
Pr-Aq-IPMC 1	32.7
Pr-Aq-IPMC 2	69.5
Pr-Aq-IPMC 3	69.0
Pr-Aq-IPMC 4	47.4

can be explained by a few different reasons. Traditionally made IPMCs that are cut into the desired dimensions from the same sheet can perform differently, even though they were manufactured at the same time, from the same membrane. This can be explained by not being able to completely control the manufacturing process of both the membranes, from the manufacturer, and the plating process, done in-house. Though a detailed procedure is followed, the entire sheet of IPMC may not be able to perform uniformly. A similar effect can be explained for the printed samples. Though we are printing the same file several times in a row, every aspect of the printing process cannot be controlled. The adhesion between the layers can differ from very good connections to not if the printer bed has shifted. Though the membranes were left in the activation bath for several hours to ensure they have been completely activated, there is a potential issue that the membranes were not fully activated. The plating process

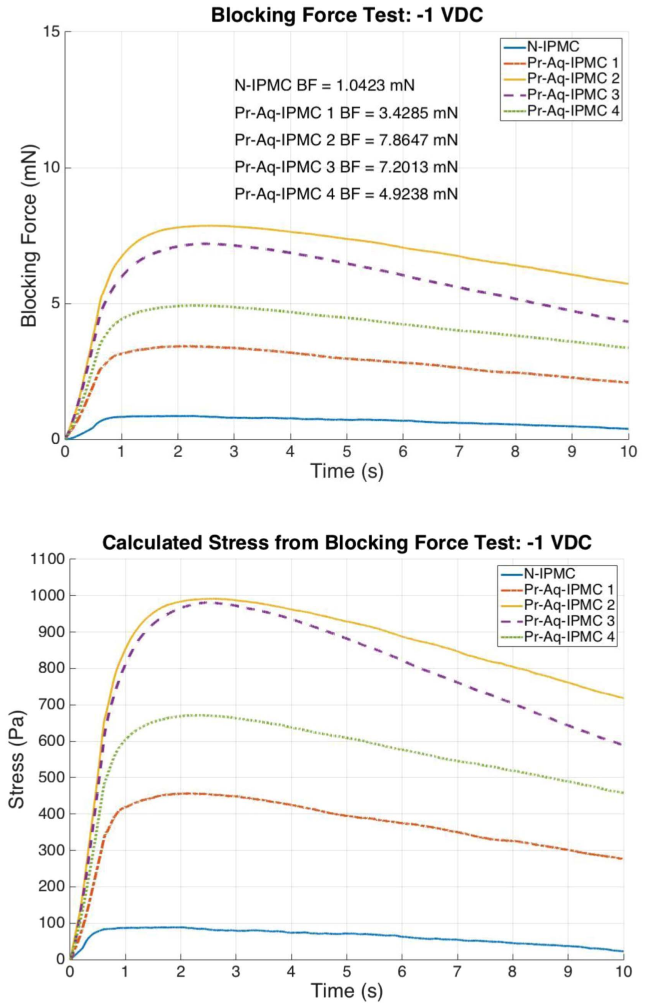

Figure 27. Blocking force tests for the IPMC samples with an applied voltage of −1 Volts DC (top) and the calculated stress from the results (bottom).

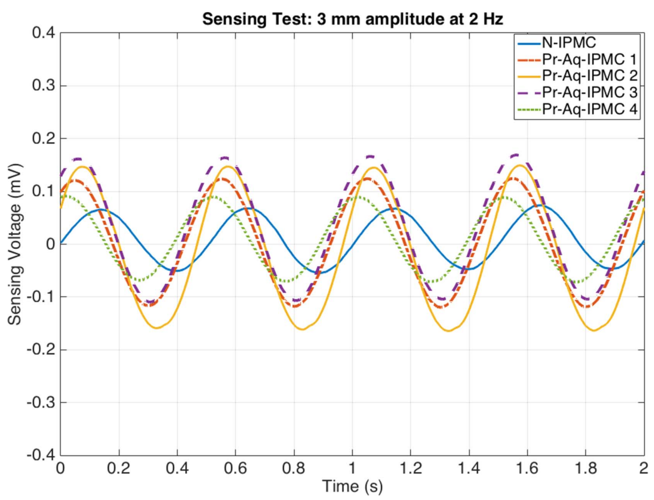

Figure 28. Sensing data from oscillating the IPMC samples with input of 3 mm (peak to peak amplitude) at 2 Hz.

though very carefully conducted, may not have evenly plated onto the surface, due to the unique surface texture of the printed samples. All of these factors could contribute to the difference in performance by each Pr-Aq-IPMC.

One aspect to note is the difference in peak to peak amplitude observed in figures 10 and 25. In figure 10, the difference between the A-IPMC and N-IPMC peak to peak amplitude is small, but noticeable. In figure 25, the peak to peak amplitude difference is much more noticeable. To explain this phenomenon, it is should be noted that typically, very thin IPMCs will have large displacements, while thicker IPMCs will actuate less. The samples in figure 10 have a thickness of about 120 μm, so they are able to have large actuations. The N-IPMC in figure 25 has a thickness of about 600 mm, which is fairly thick for an IPMC. It actuates as expected, around 2 mm peak to peak. The Pr-Aq-IPMC samples are about the same thickness, but are able to out-perform the traditional N-IPMC. This is most likely due to its high ionic conductivity, allowing the smart material to move more ions than the N-IPMC sample. The Pr-Aq-IPMC samples were able to overcome the hindrance of their large thickness.

6. Conclusions and future work

The work in this paper introduces Aquivion as a potential candidate for additive manufacturing of ionomeric polymers for the application of IPMCs. Aquivion was characterized and shown to have similar material properties to Nafion in general other than the ionic conductivity, where Aquivion has nearly double that of Nafion. This difference shows when N-IPMC and A-IPMC were tested for their performance in frequency driven actuation, with the A-IPMC performing better. Two 3D printers were modified to successfully print Aquivion filament. It was noted that the Lulzbot Mini was able to print consistently, without buckling issues. The printed membranes were activated and plated with platinum using an electroless process. The Pr-Aq-IPMC samples performed better to N-IPMC in back relaxation and strain production. In frequency driven actuation, the Pr-Aq-IPMC samples shows promise in its ability to respond faster and larger peak to peak amplitude. The Pr-Aq-IPMC samples is also able to generate a large blocking force before starting to back relax. Sensing tests showed promise for the application of Pr-Aq-IPMCs as sensors since they were able to perform better than the N-IPMC. Overall, it can be clearly seen that Aquivion is a valid option for additive manufacturing. Future work includes studying the relationship between viscosity and temperature, expanding the shapes printed into 3D structures and studying the effects of printing asymmetric shapes on actuation and mechano-electric sensing performance.

Acknowledgments

This material is based upon work supported in part by the National Science Foundation under Grant No. #1545875 (3D printing; ST, ZO, and KJK). Also, this work was supported in part by the Department of Energy Minority Serving Institution Partnership Program (MSIPP) managed by the Savannah River National Laboratory under SRNS contract TOA#0000332975 (robotics perspectives; KJK). Additionally, KJK acknowledges the partial financial support from the Office of Naval Research (N00014-16-1-2356; IPMC characterization; KJK). The authors would also like to thank Dr Hyeunhwan An for assisting in the Ion Exchange Capacity tests.

ORCID iDs

Sarah Trabia https://orcid.org/0000-0002-2598-1998
Zakai Olsen https://orcid.org/0000-0002-4499-6677
Kwang J Kim https://orcid.org/0000-0003-2134-4964

References

[1] Shahinpoor M, Bar-Cohen Y, Simpson J O and Smith J 1998 Ionic polymer–metal composites (IPMCs) as biomimetic sensors, actuators and artificial muscles—a review *Smart Mater. Struct.* **7** R15–30
[2] Shahinpoor M and Kim K J 2001 Ionic polymer metal composites: I. Fundamentals *Smart Mater. Struct.* **819** 819–33
[3] Shahinpoor M and Kim K J 2005 Ionic polymer–metal composites: IV. Industrial and medical applications *Smart Mater. Struct.* **14** 197–214
[4] Shahinpoor M and Kim K J 2004 Ionic polymer–metal composites: III. Modeling and simulation as biomimetic sensors, actuators, transducers, and artificial muscles *Smart Mater. Struct.* **13** 1362–88
[5] Shahinpoor M 1992 Conceptual design, kinematics and dynamics of swimming robotic structures using ionic polymeric gel muscles *Smart Mater. Struct.* **1** 91–4
[6] Shen Q, Wang T and Kim K J 2015 A biomimetic underwater vehicle actuated by waves with ionic polymer–metal composite soft sensors *Bioinsp. Biomim.* **10** 55007
[7] Aureli M, Kopman V and Porfiri M 2010 Free-locomotion of underwater vehicles actuated by ionic polymer metal composites *IEEE/ASME Trans. Mechatronics* **15** 603–14
[8] Shen Q, Wang T, Liang J and Wen L 2013 Hydrodynamic performance of a biomimetic robotic swimmer actuated by ionic polymer–metal composite *Smart Mater. Struct.* **22** 75035
[9] Kim B, Kim D-H, Jung J and Park J-O 2005 A biomimetic undulatory tadpole robot using ionic polymer–metal composite actuators *Smart Mater. Struct.* **14** 1579–85
[10] Chen Z, Um T I and Bart-Smith H 2012 Bio-inspired robotic manta ray powered by ionic polymer—metal composite artificial muscles **3** 296–308
[11] Yim W, Lee J and Kim K J 2007 An artificial muscle actuator for biomimetic underwater propulsors *Bioinsp. Biomim.* **2** S31–41
[12] Kamamichi N, Yamakita M, Asaka K and Zhi-Wei L 2006 A snake-like swimming robot using IPMC actuator/sensor *Proc. 2006 IEEE Int. Conf. on Robotics and Automation, ICRA 2006* (Piscataway, NJ: IEEE) p 1812–7
[13] Shahinpoor M and Kim K J 2001 Design, development and testing of a multi-fingered heart compression/assist device equipped with IPMC artificial muscles *Proc. SPIE* **4329** 411–20
[14] de Gennes P G, Okumura K, Shahinpoor M and Kim K J 2000 Mechanoelectric effects in ionic gels *Europhys. Lett.* **50** 513–8
[15] Nemat-nasser S and Li J Y 2000 Electromechanical response of ionic polymer–metal composites *J. Appl. Phys.* **87** 3321–31
[16] Pugal D, Jung K, Aabloo A and Kim K J 2010 Ionic polymer–metal composite mechanoelectrical transduction: review and perspectives *Polym. Int.* **59** 279–89
[17] Abdulsadda A T and Tan X 2012 An artificial lateral line system using IPMC sensor arrays *Int. J. Smart Nano Mater.* **3** 226–42
[18] Paola B, Fortuna L, Giannone P, Graziani S and Strazzeri S 2008 IPMCs as vibration sensors *Instrumentation and Measurement Technology Conference Proceedings* pp 2065–9
[19] Chen Z, Um T I and Bart-Smith H 2012 Bio-inspired robotic manta ray powered by ionic polymer–metal composite artificial muscles *Int. J. Smart Nano Mater.* **3** 296–308
[20] Yang T and Chen Z 2015 Development of 2D maneuverable robotic fish propelled by multiple ionic polymer–metal composite artificial fins *2015 IEEE Int. Conf. on Robotics and Biomimetics (ROBIO)* (Piscataway, NJ: IEEE) p 255–60
[21] Nelson S E 2013 Feasibility study of custom manufacturing methods of ionic polymer–metal composite sensors *M.S. Thesis*
[22] Stalbaum T, Pugal D, Nelson S E, Palmre V and Kim K J 2015 Physics-based modeling of mechano-electric transduction of tube-shaped ionic polymer-metal composite *J. Appl. Phys.* **117** 114903
[23] Palmre V, Hubbard J J, Fleming M, Pugal D, Kim S, Kim K J and Leang K K 2013 An IPMC-enabled bio-inspired bending/twisting fin for underwater applications *Smart Mater. Struct.* **22** 14003
[24] Kim B, Kim B M, Ryu J, Oh I-H, Lee S-K, Cha S-E and Pak J. 2003 Analysis of mechanical characteristics of the ionic polymer metal composite (IPMC) actuator using cast ion-exchange film *Proc. SPIE* **5051** 484296
[25] Kim K and Shahinpoor M 2002 A novel method of manufacturing three-dimensional ionic polymer–metal composites (IPMCs) biomimetic sensors, actuators and artificial muscles *Polymer* **43** 797–802
[26] Hwang T, Palmre V, Nam J, Lee D-C and Kim K J 2015 A new ionic polymer–metal composite based on Nafion/poly (vinyl alcohol-co-ethylene) blends *Smart Mater. Struct.* **24** 105011
[27] Nam J, Hwang T, Kim KJ and Lee D 2017 A new high-performance ionic polymer–metal composite based on Nafion/polyimide blends *Smart Mater. Struct.* **26** 35015
[28] Trabia S, Hwang T and Kim K J 2016 A fabrication method of unique Nafion® shapes by painting for ionic polymer–metal composites *Smart Mater. Struct.* **25** 85006
[29] Carrico J D, Traeden N W, Aureli M and Leang K K 2015 Fused filament 3D printing of ionic polymer–metal composites (IPMCs) *Smart Mater. Struct.* **24** 125021
[30] Carrico J D and Leang K K 2017 Fused filament 3D printing of ionic polymer–metal composites for soft robotics *Proc. SPIE* **10163** 101630I
[31] Turner B N, Strong R and Gold S A 2014 A review of melt extrusion additive manufacturing processes: I. Process design and modeling *Rapid Prototyp. J.* **20** 192–204
[32] Elliott J A, James P J, McMaster T J, Newton J M, Elliott A M S, Hanna S and Miles M J 2001 Hydrolysis of the Nafion® precursor studied by x-ray scattering and *in situ* atomic force microscopy *e-Polymers* **1** 1–11
[33] Kim K J and Shahinpoor M 2003 Ionic polymer metal composites: II. Manufacturing techniques *Smart Mater. Struct.* **12** 65–79
[34] Zhang F, Zhang Z, Liu Y, Lu H and Leng J 2013 The quintuple-shape memory effect in electrospun nanofiber membranes *Smart Mater. Struct.* **22** 85020

[35] Ketpang K, Shanmugam S, Suwanboon C, Chanunpanich N and Lee D 2015 Efficient water management of composite membranes operated in polymer electrolyte membrane fuel cells under low relative humidity *J. Memb. Sci.* **493** 285–98
[36] Chen C and Fuller T F 2009 The effect of humidity on the degradation of Nafion® membrane *Polym. Degrad. Stab.* **94** 1436–47
[37] Zheng J, He Q, Liu C, Yuan T, Zhang S and Yang H 2015 Nafion-microporous organic polymer networks composite membranes *J. Memb. Sci.* **476** 571–9
[38] Shen L, Sun Z, Chu Y, Zou J and Deshusses M 2015 Novel sulfonated Nafion®-based composite membranes with pillararene as selective artificial proton channels for application in direct methanol fuel cells *Int. J. Hydrog. Energy* **40** 13071–9
[39] Di Noto V, Gliubizzi R, Negro E and Pace G 2006 Effect of SiO_2 on relaxation phenomena and mechanism of ion conductivity of [Nafion/$(SiO_2)_x$] composite membranes† *J. Phys. Chem.* **110** 24972–86
[40] Sha Wang L, Nan Lai A, Xiao Lin C, Gen Zhang Q, Mei Zhu A and Lin Liu Q 2015 Orderly sandwich-shaped graphene oxide/Nafion composite membranes for direct methanol fuel cells *J. Memb. Sci.* **492** 58–66
[41] Deng Q, Wilkie C A, Moore R B and Mauritz K A 1998 TGA–FTi.r. investigation of the thermal degradation of Nafion® and Nafion®/[silicon oxide]-based nanocomposites *Polymer* **39** 5961–72
[42] Khandelwal M and Mench M M 2006 Direct measurement of through-plane thermal conductivity and contact resistance in fuel cell materials *J. Power Sources* **161** 1106–15
[43] Chemours 2016 Nafion Membrane Data Sheet
[44] Solvay 2015 Aquivion® P87S-SO2F
[45] Solvay 2015 Aquivion® E87-05s
[46] Shankar R, Ghosh T K and Spontak R J 2007 Dielectric elastomers as next-generation polymeric actuators *Soft Matter* **3** 1116
[47] Moukheiber E, De Moor G, Flandin L and Bas C 2012 Investigation of ionomer structure through its dependence on ion exchange capacity (IEC) *J. Membr. Sci.* 294–304